Effect of the Silo-Bottom Design on the Granular Behaviour during Discharging Process

WARIAM CHUAYJAN
Thaksin University (Phatthalung Campus)
Department of Mathematics, Faculty of Science, Phatthalung 93110
Centre of Excellence in Mathematics, PERDO, CHE, Bangkok 10400
THAILAND
cwariam@tsu.ac.th

PICHIT BOONKRONG
Mahidol University
Department of Mathematics
Centre of Excellence in Mathematics
PERDO, CHE, Bangkok 10400
THAILAND
pijiito@gmail.com

BENCHAWAN WIWATANAPATAPHEE*
Mahidol University
Department of Mathematics
Centre of Excellence in Mathematics
PERDO, CHE, Bangkok 10400
THAILAND
scbww@mahidol.ac.th

Abstract: This paper aims to investigate the effect of the silo-bottom design on the dynamic behaviour of granular flow during discharging process in a varied mass-flow silo. Three different designs of hopper bottom including a flat-bottomed silo, a cylinder-hopper silo and a silo with double-opening bottom are considered. We assume that the granular material is an assembly of 10,000 soybeans. Governing equations including the principle of linear momentum and angular momentum describes the motion of particles. Discrete element method is manipulated for the solution of the governing equations. The simulation results indicate that Zig-Zag flow occurs in the cylinder-hopper silo and the silo with double-opening bottom. Comparing with other silos, arching and low pressure occur in a double-opening bottom silo whereas dead zone and high pressure appear in the flat-bottomed silo.

Key–Words: mathematical modelling, discrete element method, granular flow, flat-bottomed silo, cylinder-hopper silo, silo with double-opening bottom.

1 Introduction

In soybean industries, there are many problems encountered during the filling and discharging processes. The problems are mainly the formation of stable arch formed above the hopper outlet, the piping or dead zone occurring near the silo wall and the segregation due to variety of particle sizes. Moreover, a misappropriate design of silo usually causes silo collapse that brings lots of damage. To overcome the problem, understanding fully the physics of granular flow is needed. Over the past two decades, extensive studies based on experiments and numerical models have been carried out to study the characteristic of granular flow in silos. In the experimental models, pressure distribution in silo have been measured. Janssen (1895) firstly reported the pressure distribution at the bottom of the silo [2]. Jenike (1964) studied the importance of characterising the flow of granular material during discharging process of a silo and investigated its effect on the wall pressure distribution [3]. Thereafter, Aoki and Tsunakawa (1969) measured wall pressure distribution in a hopper and a bin-hopper system under stationary and flowing conditions [4]. They found that the material bed near the outlet becomes loose under gravity flow condition and the velocity of individual particles rapidly escalated. Subsequently, the dynamic pressure on the wall continuously rose. Afterwards, a number of mathematical models of granular flow in a silo have been proposed to analyse the effect of relevant factors such as bottom angle and outlet width, inlet flow rate and particle shape [8, 9, 10, 11, 12, 13, 14, 15]. According to the curiosity in flow pattern of granular materials in silo, three well-known methods which are hybrid method, Discrete Element Method (DEM) and Finite Element Method (FEM) have been widely applied to investigate the flow behaviour of granular solids and the pressure distribution in silos. Masson and Martinez

*Corresponding author

(2002) investigated the effect of particle properties and silo geometry using DEM [5] . They used a flat-bottomed silo and a cylinder-hopper silo, containing 10,000 and 8,500 particles in simulation. Their results showed that both mechanical properties of the granular solids, namely contact stiffness and friction play a major role on the force transmission patterns, and more specifically on arching effects. Li et al. (2004) studied three-dimensional flow of granular particles in a rectangular hopper using both experiment and DEM [6]. In their experiment, the particle flow behaviour, arching effects and the measurement of particle mass flow rate at three different hopper openings were taken into account using high-speed video recording analysis. The results indicated that DEM can be used to analyse particle packing structure and flow patterns more thoroughly than the experiment. Afterward, Wu et al. (2009) performed a multi-scale study of the particle flow by means of DEM [7]. They investigated the flow behaviours on the particles diameter distribution and silo geometry to establish the spatial and statistical distributions of micro-dynamic variables related to flow and silo structures. The results showed that the distribution of particle diameter has higher impacts on particle flow. The silo geometry has greater effects on granular flow than particle size distribution and inserts can improve the flow behaviour of funnel flow type to mass flow.

The aforementioned studies have influenced on the basic understanding of granular flow and have basically guided how to design a suitable silo for each industry. Nevertheless, the general problems such as the formation of arching, dead zone and Zig-Zag flow in the silo have not been clearly understood nor well controlled. Thus, further study of the filling and discharging processes is still interesting as the development of appropriate mathematical models. Besides, numerical technique becomes an important tool for the simulation of granular flow and the design of new silo systems as well as the optimisation of these processes.

In this paper, we extend our previous work based on DEM [1]. It is devoted on the study of granular flow during discharging process in three different designs of silo bottom including a flat-bottomed silo, a cylinder-hopper silo and a silo with double-opening bottom. The mathematical model of granular flow is illustrated in section 2. In section 3, the effect of the bottom designs on the flow pattern and pressure distribution are investigated in the form of numerical example, and conclusion is given in section 4.

2 Mathematical Model

Based on the assumption that all physically mechanical properties of granular materials are the same. The governing equations of particle flow model describing the translational and rotational motions become the principle of linear and angular momentums, namely

$$m_i \frac{d\mathbf{v}_i(t)}{dt} = \mathbf{F}_i(t) + m_i \mathbf{g}, \tag{1}$$

$$I_i \frac{d\boldsymbol{\omega}_i(t)}{dt} = M_i(t), \tag{2}$$

where $\mathbf{v}_i$ and $\boldsymbol{\omega}_i$ are the linear and angular velocities at the centre of the i^{th} particle; m_i and I_i respectively denote the mass and the moment of inertia of the particle; $\mathbf{F}_i(t)$ is the total force due to interaction between particle-particle and particle-wall. $\mathbf{F}_i(t)$ in equation (1) is the sum of normal force and tangential force and the M_i in equation (2) is due to tangential torque causing a particle to rotate. To simulate the granular flow during discharging process, we introduce two new variables:

$$\mathbf{v}_i = \frac{d\mathbf{r}_i(t)}{dt}, \tag{3}$$

$$\boldsymbol{\omega}_i = \frac{d\boldsymbol{\theta}_i(t)}{dt}. \tag{4}$$

where $\mathbf{r}_i$ and $\boldsymbol{\theta}_i$ are the position and the rotation vectors such that

$$\begin{aligned} \mathbf{r}_i(t) &= [r_1(t), r_2(t), \ldots, r_N(t)]^T, \\ \boldsymbol{\theta}_i(t) &= [\theta_1(t), \theta_2(t), \ldots, \theta_N(t)]^T. \end{aligned}$$

Assembling the equation of all particle motions yields a system of $8N$ first order differential equations in 2-D case, namely

$$\dot{\mathbf{z}}(t) = \mathbf{w}(t), \tag{5}$$

$$\dot{\mathbf{w}}(t) = \mathbf{P}(t), \tag{6}$$

where

$$\begin{aligned} \mathbf{z}(t) &= [\mathbf{r}_1(t), \boldsymbol{\theta}_1(t), ..., \mathbf{r}_N(t), \boldsymbol{\theta}_N(t)]^T, \\ \mathbf{w}(t) &= [\mathbf{v}_1(t), \boldsymbol{\omega}_1(t), ..., \mathbf{v}_N(t), \boldsymbol{\omega}_N(t)]^T, \\ \mathbf{P} &= \left[\frac{\mathbf{F}_1}{m_1} + \mathbf{g}, \frac{M_1}{I_1}, ..., \frac{\mathbf{F}_N}{m_N} + \mathbf{g}, \frac{M_N}{I_N}\right]^T. \end{aligned}$$

3 Numerical Example

From section 2, we have presented the mathematical model based on the DEM and numerical scheme. A numerical study has been conducted to analyse the effects of the hopper bottom on the flow behaviour in the dynamic process of material discharging of a silo. In our experiment, the examples under consideration include a flat-bottomed silo, a cylinder-hopper silo and a silo with double-opening bottom. Each silo is made of a steel-sheet with the height of $1.3\,m$ and the width of $0.4\,m$. As can be seen in Figure 1, the three different geometries of silo are designed and are then used as the computational region. The flat-bottomed silo and the cylinder-hopper silo have the same outlet width of $0.08\,m$ whilst a silo with double-opening bottom has $0.04\,m$ of the left and the right outlets width. The hopper angles (α) of the flat-bottomed silo, cylinder-hopper silo and silo with double-opening bottom are $0°$, $45°$ and $45°$, respectively. Granular materials are assumed to be two different sizes of spherical particles which are $0.006\,m$ and $0.0075\,m$.

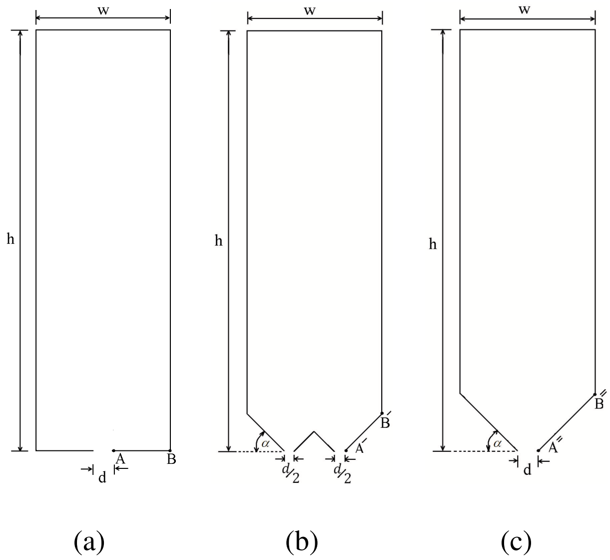

Figure 1: Geometries of the silo including (a) flat-bottomed silo; (b) silo with a double-opening bottom and (c) cylinder-hopper silo.

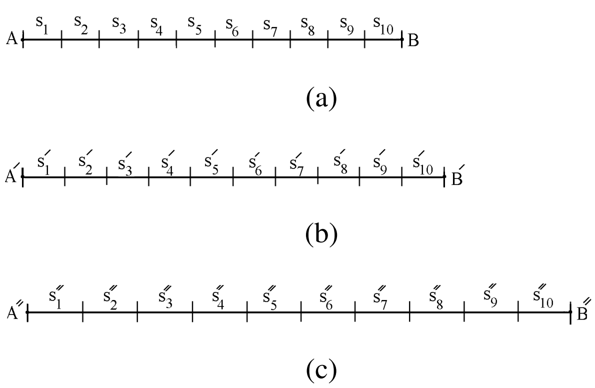

Figure 2: Wall segments of the silo bottom: (a) flat-bottomed silo; (b) silo with a double-opening bottom and (c) cylinder-hopper silo.

Table 1 shows the model parameters used to the determine the velocity field and pressure field throughout the simulation and Table 2 shows properties of particle including normal contact stiffness, tangential contact stiffness, normal damping constant and frictional coefficient.

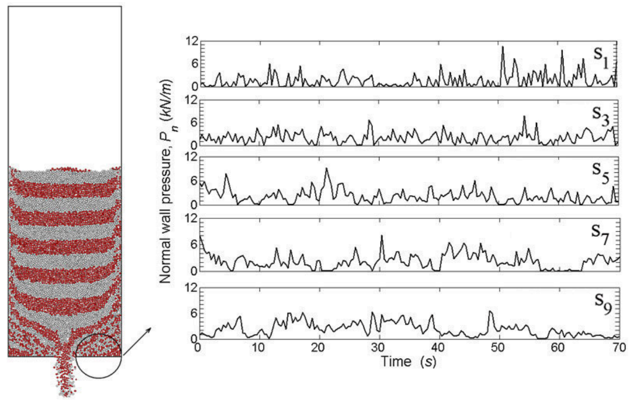

Figure 3: The variation of the normal pressure with time along five hopper-wall segments in the flat-bottomed silo.

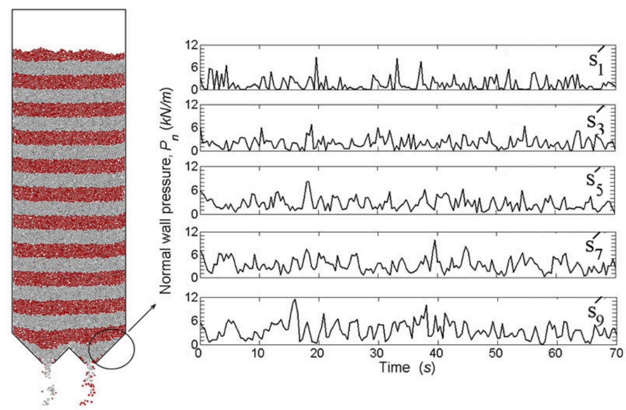

Figure 4: The variation of the normal pressure with time along five hopper-wall segments in the silo with double-opening bottom.

To study the dynamic process of granular flow during discharging process in a varied mass-flow silo, the assembly of $10,000$ particles are allowed to flow out of the silo under gravitational force at the beginning time $t = 0\,s$. To investigate pressure distribution on the hopper bottom, we have recorded the pressure distribution on the hopper bottom at 10 segments as displayed in Figure 2. The investigated variation of normal pressure acting on five segments of those hopper-bottomed designs are shown in Figures 3, 4 and 5. It is found that the high pressure occurs in the segments close to outlets.

Table 1: Parameter values used in simulation

Parameters	Values
particle diameter, (mm)	6 and 7.5
particle density, $\rho\,(kg/m^3)$	$1,033$
number of particles with size of $6\,mm$	$3,500$
number of particles with size of $7.5\,mm$	$4,000$
silo height, $h\,(m)$	1.3
silo width, $w\,(m)$	0.4
simulation time step, $\triangle t\,(s)$	5.2711×10^{-6}

Table 2: Properties of particle

Properties	Particle-particle	Particle-wall
normal contact stiffness, $k_n\,(N/m)$	2.8322×10^4	5.6645×10^4
tangential contact stiffness, $k_s\,(N/m)$	2.5740×10^4	4.5314×10^4
normal damping constant, $\eta_n\,(N/m)$	1.3048×10^2	1.3962×10^2
frictional coefficient, μ	0.33	0.35

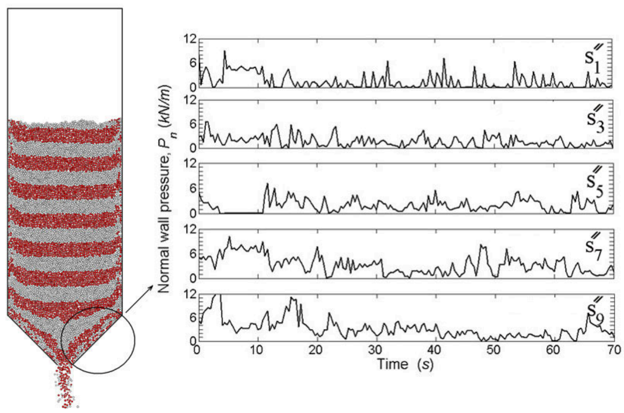

Figure 5: The variation of the normal pressure with time along five hopper-wall segments in the cylinder-hopper silo.

In order to investigate the flow pattern in silos, the particles are coloured into layers using two colours. The three different computational regions have been used in computation for investigating the flow pattern, the deformation of the interfaces and the wall pressure in silos. Figures 6, 7 , 8 and 9 present the computed flow pattern, the arching, the velocity field, and the wall pressure, respectively. The results indicate that Zig-Zag flow occurs in the cylinder-hopper silo and the silo with double-opening bottom. It is remarkable that the flow rate of particles in a flat-bottomed silo is the highest, but dead zones gradually form around its corners. Eclectically, arching occurs in both of the left and the right outlets of a double-opening bottom silo. At time $t = 4.7\,s$, the arching occurs above the right outlet and block the flow of the particles, until it cannot block the flow at time $t = 13\,s$ and particles start to flow out from the right outlet again. After that, the stable arch is formed over the left outlet at time $t = 18\,s$. Finally, the stable arch is formed over the right outlet at time $t = 100\,s$. Alternatively, formation of arching switches between the left and the right outlets during the simulation. This formation causes the delay in discharging process.

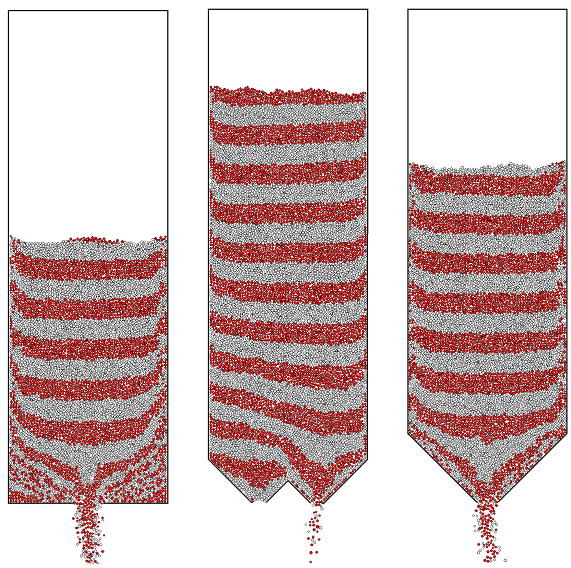

(a) (b) (c)

Figure 6: Effect of the hopper shape on discharge pattern at $t = 75\,s$: (a) a flat-bottomed silo; (b) a silo with double-opening bottom and (c) a cylinder-hopper silo.

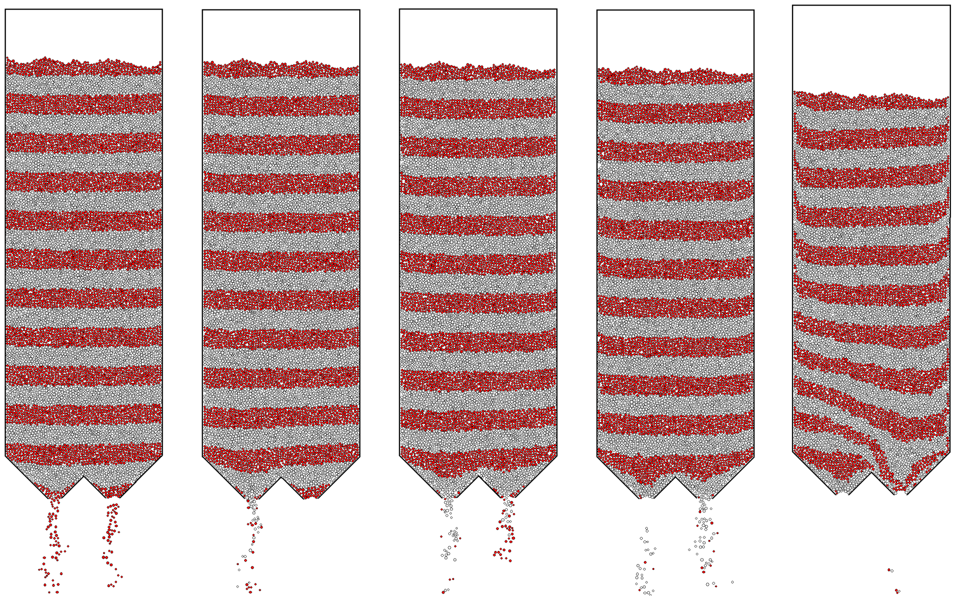

(a) $t = 5\,s$ (b) $t = 10\,s$ (c) $t = 15\,s$ (d) $t = 20\,s$ (e) $t = 105\,s$

Figure 8: The formation of arching above the outlet in a silo with double-opening bottom at different times.

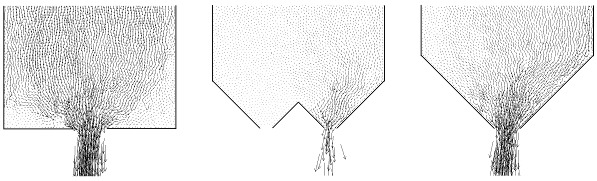

(a) (b) (c)

Figure 7: Velocity field of granular materials in silo with three different designs of hopper bottom at $t = 75\,s$: (a) a flat-bottomed silo; (b) a silo with double-opening bottom and (c) a cylinder-hopper silo.

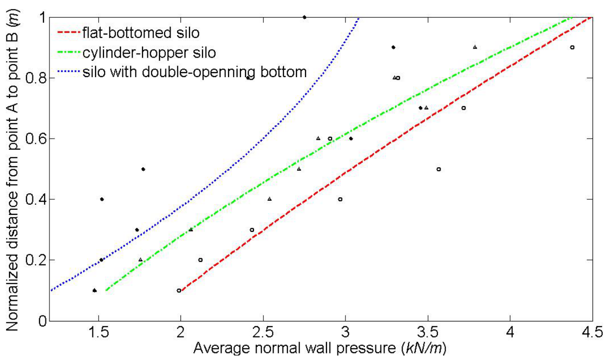

Figure 9: Average normal pressure along the bottom wall (from point A to B in Figure 1) during the first $70\,s$ of discharge process under the three different shapes of the hopper.

The influence of the three different shapes of the hopper on the bottom wall pressure is investigated for the varied mass-flow silo. The comparison of computed average normal wall pressure for three different shapes of the hopper is shown in Figure 9. The results show that the average normal wall pressures in those three silos seem to linearly increase. The maxima of the average normal wall pressure occurs in the flat-bottomed silo whilst the minima appears in the silo with double-opening bottom.

4 Conclusion

The dynamic behaviour of granular materials draining inside three types of silo are studied via mathematical model using DEM and numerical simulation. The marked differences among silo geometries affect the flow pattern of granular materials and pressure on the silo bottom. That is, Zig-Zag flow happens in the cylinder-hopper silo and the silo with double-opening bottom, and arching forms in the double-opening bottom silo. The average normal wall pressure in the double-opening bottom silo is the lowest whilst the pressure in the flat-bottom is the highest. Still, it is clear that further work is also needed to develop the appropriate silo for each industry.

Acknowledgments: The first author gratefully acknowledges the financial support from the Centre of Excellence in Mathematics, CHE, Ministry of Education, THAILAND.

References:

[1] W. Chuayjan, S. Pothiphan, B. Wiwatanapataphee and Y.H. Wu, Numerical simulation of granular flow during filling and discharging of a silo, *International Journal of Pure and Applied Mathematics.* 62(3), 2010, pp. 347–364.

[2] H.A. Janssen, Test on grain pressure in silos, *Zeitschrife des Vereines Deutscher Ingenieure* 39, 1895, pp. 243–254.

[3] A.W. Jenike, Storage and flow of solids, *Bul. 123, Utah Engineering Expt. Sta. Univ. of Utah*, 1895.

[4] R. Aoki and H. Tsunakawa, The prssure in a grnular material at the wall of bins and hoppers, *J. of Chemical Engineering of Japan.* 2, 1969, pp. 126–129.

[5] S. Masson and J. Martinez, Effect of particle properties and silo geometry on stresses predicted by discrete simulations of bulk materials, 15^{th} *ASCE Engineering Mechanics Conference.* 2-5, 2002, pp. 1–8.

[6] J. Li, P.A. Langston, C Webb and T. Dyakowski, Flow of sphero-disc particles in rectangular hoppers a DEM and experimental comparision in 3D, *Chemical Engineering Science.* 59, 2004, pp. 5917–5929.

[7] J. Wu, J. Binbo, J. Chen and Y. Yang, Multi-scale study of particle flow in silos, *Advanced Power Technology.* 20, 2009, pp. 62–73.

[8] P.A. Cundall and O.D.L. Strack, Discrete numerical model for granular asemblies, *Geotechnique.* 29, 1979, pp. 47–65.

[9] R.J. Goodey, C.J. Brown and J.M. Rotter, Predicted patterns of filling predures in thin-walled square silos, *Engineering Structures.* 28, 2006, pp. 109–119.

[10] T. Karlsson, M. Klisinski and K. Runesson, Finite element simulation of granular material flow in plane silos with complicated geometry, *Powder Techology.* 99, 1998, pp. 29–39.

[11] P.A. Langston, U. Tuzu and D.M. Heyes, Discrete element simulation of granular flow in 2D and 3D hoppers dependence of discharge rate and wall stress on particle interactions, *Chemical Engineering Science.* 50, 1995a, pp. 967–979.

[12] P.A. Langston, U. Tuzu and D.M. Heyes, Discrete element simulation of internal-stress and flow-fileds in funnel flow hoppers, *Powder Technology.* 85, 1995b, pp. 153–169.

[13] J. Li, P.A. Langston, C. Webb and T. Dyakowski, Flow of sphero-disc particles in rectangular hoppers a DEM and experimental comparision in 3D, *Chemical Engineering Science.* 59, 2004, pp. 5917–5929.

[14] J.M. Rotter, C.J. Brown and E.H. Lahlouh, Patterns of wall pressure on filling a square planform steel silo, *Engineering Structures.* 24, 2002, pp. 135–150.

[15] G.H. Ristow, *Pattern Formation in Granular Materials,* Springer – New Yorko 2000